Hot electron relaxation and energy loss rate in silicon: Temperature dependence and main scattering channels

View Online   Export Citation   CrossMark

R. Sen, (iD) N. Vast, and J. Sjakste[a]) (iD)

AFFILIATIONS

Laboratoire des Solides Irradiés, CEA/DRF/IRAMIS, École Polytechnique, CNRS, Institut Polytechnique de Paris, 91120 Palaiseau, France

[a])Author to whom correspondence should be addressed: jelena.sjakste@polytechnique.edu

ABSTRACT

In this work, we revisit the density functional theory (DFT)-based results for electron–phonon scattering in highly excited silicon. Using the state-of-the-art *ab initio* methods, we examine the main scattering channels, which contribute to the total electron–phonon scattering rate and the energy loss rate of photoexcited electrons in silicon as well as their temperature dependence. Both temperature dependence and the main scattering channels are shown to strongly differ for the total electron–phonon scattering rate and the energy loss rate of photoexcited electrons. While the total electron–phonon scattering rate increases strongly with temperature, the temperature dependence of the energy loss rate is negligible. Also, while acoustic phonons dominate the total electron–phonon scattering rate at 300 K, the main contribution to the energy loss rate comes from optical modes. In this respect, DFT-based results are found to disagree with conclusions of Fischetti *et al.* [Appl. Phys. Lett. **114**, 222104 (2019)]. We explain the origin of this discrepancy, which is mainly due to differences in the description of the electron–phonon scattering channels associated with transverse phonons.

Published under an exclusive license by AIP Publishing. https://doi.org/10.1063/5.0082727

Although apparently well-studied,[1–6] electron–phonon coupling in silicon continues to attract attention from both experimental and theoretical points of view[7,8] and even to arouse debate.[9] One of the reasons for this continuing interest is the outmost importance of the electron–phonon coupling in silicon for simulation of transport in numerous devices.[10,11]

In the present work, we examine, using methods based on the density functional theory (DFT), temperature dependence and the main scattering channels of the energy loss rate of photoexcited electrons in silicon due to the electron–phonon scattering. For photoexcited carriers, one can identify two distinct relaxation regimes, both determined by the electron–phonon scattering: one is related to the loss of the initial momentum (redistribution of carriers in the Brillouin zone) and the other to the energy transfer from electrons to phonons.[12,13]

Recently, the rate of energy transfer from electrons to phonons in silicon (referred to as the energy relaxation rate in Refs. 8, 12, and 13 and energy loss rate in other works[14]) has been measured by a two-photon photoemission experiment over a large range of photoexcited electron energies, at 300 K, and found in good agreement with DFT-based calculations.[8] However, the temperature dependence of the energy transfer rate has not been examined in Ref. 8. Moreover, the

main scattering channels responsible for energy transfer from electrons to phonons in silicon have been discussed recently in Ref. 9, and, surprisingly, it has been concluded that the energy of hot electrons is mostly lost by transfer to acoustic phonons, contrarily to common belief.[14] In this work, we will clarify the positioning of DFT results with respect to the main channels of the energy transfer from electrons to phonons.

This Letter is organized as follows: First, we will present very briefly the technical details of our calculations and remind the reader of the definition of the energy transfer rate from electrons to phonons. Then, we will present the DFT results for the temperature dependence of the energy transfer rate and the main electron–phonon scattering channels, which contribute to the energy transfer. Finally, we will discuss the main differences between the electron–phonon coupling parameters obtained by DFT and the ones used in Monte Carlo (MC) simulations of Ref. 9, in order to clarify the origin of the discrepancy in the identification of the main scattering channels.

The total electron–phonon scattering rate, or self-energy, is implemented, e.g., in the EPW code[15] and defined in numerous other works[13,16,17]

$$\tau_{n\mathbf{k}}^{-1} = \Gamma_{em} + \Gamma_{abs}, \qquad (1)$$

where

$$\Gamma_{em} = \frac{2\pi}{\hbar} \Sigma_{m\nu} \int \frac{d\mathbf{q}}{\Omega_{BZ}} |g_{mn\nu}(\mathbf{k},\mathbf{q})|^2$$
$$\times (N_{\mathbf{q},\nu} + 1 - f_{m,\mathbf{k}+\mathbf{q}}) \delta(\varepsilon_{n,\mathbf{k}} - \varepsilon_{m,\mathbf{k}+\mathbf{q}} - \hbar\omega_{\mathbf{q}\nu}),$$

$$\Gamma_{abs} = \frac{2\pi}{\hbar} \Sigma_{m\nu} \int \frac{d\mathbf{q}}{\Omega_{BZ}} |g_{mn\nu}(\mathbf{k},\mathbf{q})|^2$$
$$\times (N_{\mathbf{q},\nu} + f_{m,\mathbf{k}+\mathbf{q}}) \delta(\varepsilon_{n,\mathbf{k}} - \varepsilon_{m,\mathbf{k}+\mathbf{q}} + \hbar\omega_{\mathbf{q}\nu}). \qquad (2)$$

Here, all emission and absorption processes allowed by energy and momentum conservation are taken into account. $g_{mn\nu}(\mathbf{k},\mathbf{q})$ stand for the electron–phonon matrix elements between electronic states with m and n band numbers, coupled via the phonon mode ν. $N_{\mathbf{q},\nu}$ stand for phonon population numbers (Bose-Einstein distribution), $f_{n,\mathbf{k}}$ is the electron Fermi–Dirac distribution function, $\varepsilon_{n,\mathbf{k}}$ are electron eigenenergies, and $\omega_{\mathbf{q}\nu}$ are phonon frequencies. The total electron–phonon scattering rate expresses the probability for an excited electron to change its initial momentum, i.e., to be scattered elsewhere in the Brillouin zone, it was referred to as "momentum scattering rate" in some of our previous works.[12,13,18]

The energy relaxation rate, or, equivalently, the rate of energy transfer to phonons, reads[13,14,16]

$$\frac{\delta E}{\delta t} = \Gamma_{em}\omega_{em} - \Gamma_{abs}\omega_{abs}$$
$$= \frac{2\pi}{\hbar} \Sigma_{m\nu} \int \frac{d\mathbf{q}}{\Omega_{BZ}} \omega_{\mathbf{q}\nu} |g_{mn\nu}(\mathbf{k},\mathbf{q})|^2$$
$$\times (N_{\mathbf{q},\nu} + 1 - f_{m,\mathbf{k}+\mathbf{q}}) \delta(\varepsilon_{n,\mathbf{k}} - \varepsilon_{m,\mathbf{k}+\mathbf{q}} - \hbar\omega_{\mathbf{q}\nu})$$
$$- \frac{2\pi}{\hbar} \Sigma_{m\nu} \int \frac{d\mathbf{q}}{\Omega_{BZ}} \omega_{\mathbf{q}\nu} |g_{mn\nu}(\mathbf{k},\mathbf{q})|^2$$
$$\times (N_{\mathbf{q},\nu} + f_{m,\mathbf{k}+\mathbf{q}}) \delta(\varepsilon_{n,\mathbf{k}} - \varepsilon_{m,\mathbf{k}+\mathbf{q}} + \hbar\omega_{\mathbf{q}\nu}). \qquad (3)$$

In this work, we used the method of calculation of the electron–phonon matrix elements based on the density functional perturbation theory (DFPT)[19,20] and interpolation in the Wannier space.[15,21] We used both the EPW code[15] and the independent implementation of Ref. 21 with identical results. Our DFT calculations were performed within the local density approximation (LDA). All technical details of our calculations are provided in the supplementary material.

While the total electron–phonon scattering rate involves the sum of emission and absorption probabilities over all possible final states, the rate of energy transfer to phonons involves, contrastingly, the difference between emission and absorption[13,14,16] [see Eqs. (1)–(3)].

In Fig. 1, we show the comparison between the total electron–phonon scattering rate (top panel) and energy transfer rate (bottom panel) for silicon as a function of the electron excess energy, at 300 K and at 0 K. In Fig. 1, we have considered the initial electronic states along the $\Gamma - X$ direction in the Brillouin zone (see the supplementary material, Sec. I E). As one can see in Fig. 1 (upper panel), our calculated total scattering rates of hot electrons in silicon (at 300 K) are found in close agreement with the work of Fischetti et al.[9] as well as with our previous work,[8] in which a different implementation of the Wannier interpolation of the electron–phonon matrix elements was used.[21] Also, the results of Ref. 4 (not shown in Fig. 1) are very close to the ones presented here. The results of Ref. 8 are shown in order to
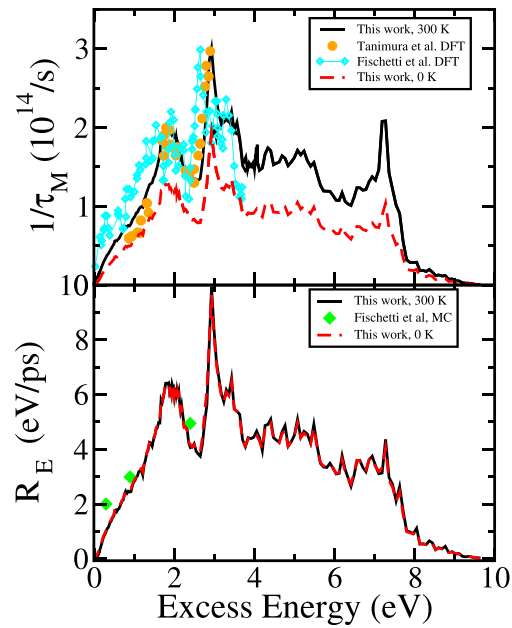

FIG. 1. Upper panel: Total electron–phonon scattering rate of hot electrons in silicon, at 300 and 0 K. Initial state along the $\Gamma - X$ direction in the Brillouin zone. The theoretical DFT-based results from Refs. 8 and 9 at 300 K are also shown. Lower panel: Energy loss rate from electrons to phonons, at 300 K and 0 K. The results obtained by the Monte Carlo simulation method from Ref. 9 at 300 K are also shown. (The correspondence between field and excess energy was taken from Ref. 11.)

demonstrate that different implementations of the Wannier interpolations yield the same results, as expected. The calculated energy loss rates of hot electrons at 300 K are shown in the lower panel of Fig. 1. As one can see in the lower panel of Fig. 1, DFT-based energy loss rates are found to be close to the energy loss rates obtained by MC simulations in Ref. 9.

The upper panel of Fig. 1 demonstrates that the total electron–phonon scattering rate grows strongly with temperature due to the growing populations of acoustic phonons. In contrast, as shown in the lower panel of Fig. 1, the energy transfer rate is found to be essentially independent of temperature, as the changes due to temperature in both emission and absorption contributions cancel each other. It must be noted that in the case of GaAs,[13] the energy transfer rate was even found to decrease with growing temperature (see Note 1 in the supplementary material).

In Figs. 2 and 3, we analyze the contributions of the optical and acoustic modes to the total electron–phonon scattering rate and to the energy transfer rate. Recently, Fischetti et al.[9] have discussed the relative contributions of the electron–phonon scattering channels involving optical and acoustic phonons to the energy loss rate of hot electrons in silicon. The discussion was mainly based on the results of MC simulations,[11] coupled to effective electron–phonon coupling constants, which were obtained by a fit of the experimental data. However, DFT calculations were also mentioned: Fischetti et al. performed DFT-based calculations of the total electron–phonon scattering rates for the hot electrons as a function of the excess energy at room temperature. These calculations demonstrated that at room
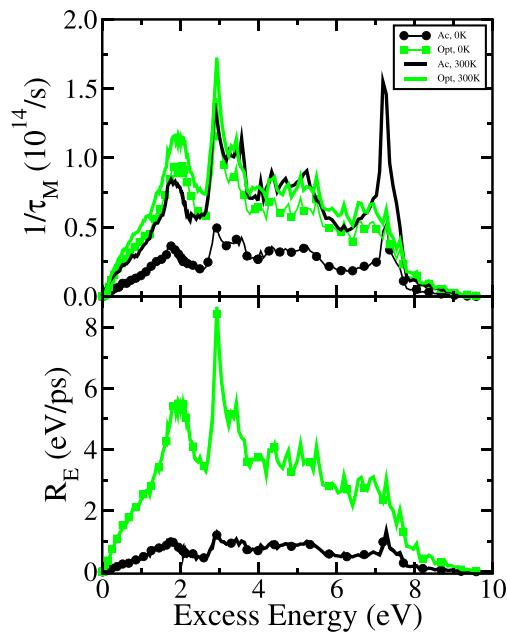
FIG. 2. Contributions of the acoustic and optical channels to the total electron–phonon scattering rate and to the energy loss rate of hot electrons in silicon, at 0 K and at 300 K. Initial state along the $\Gamma - X$ direction in the Brillouin zone. Upper panel: Acoustic and optical phonon contributions to the total electron–phonon scattering rate. Thick solid lines: acoustic (black) and optical (green) contributions to the total electron–phonon scattering rate at 300 K. Symbols with thin lines: acoustic (black circles) and optical (green squares) contributions to the total electron–phonon scattering rate at 0 K. Lower panel: Acoustic and optical phonon contributions to the energy loss rate. Thick solid lines: acoustic (black) and optical (green) contributions to the energy loss rate at 300 K. Symbols with thin lines: acoustic (black circles) and optical (green squares) contributions to the energy loss rate at 0 K.

FIG. 3. Contributions of the acoustic (black squares) and optical (green diamonds) channels to the total electron–phonon scattering rate and to the energy loss rate of hot electrons in silicon, at 300 K. Results averaged over the initial electronic states belonging to the constant energy isosurfaces of varying excess energy. Upper panel: Acoustic and optical phonon contributions to the total electron–phonon scattering rate. Lower panel: Acoustic and optical phonon contributions to the energy loss rate.

temperature, the acoustic phonons play a dominant role in the total electron–phonon scattering rate. These data provided an additional argument, which led the authors of Ref. 9 to the conclusion that the DFT result agrees with their previous calculations of Ref. 11, and that, contrarily to the common belief, both theoretical approaches supposedly indicated that the energy of hot electrons is mostly lost by transfer to acoustic phonons. Here, we clarify the positioning of the DFT results with respect to this issue.

First, we note that we find the contribution of the acoustic phonons to the total scattering rate of hot electrons at 300 K to be comparable to that of the optical phonons when the initial states are considered along the $\Gamma - X$ direction (Fig. 2, upper panel, solid lines). Moreover, we find the contribution of the acoustic phonons to be the dominant one when considering the results averaged over the initial electronic states belonging to the constant energy isosurfaces (Fig. 3, upper panel) in agreement with Fischetti et al. However, in contrast to room temperature results, at 0 K, the contribution of the optical phonons to the total scattering rate is found to be the largely dominant one (Fig. 2, upper panel, symbols). Therefore, the dominant role of the acoustic phonons in the total electron–phonon scattering rate of hot electrons in silicon at 300 K predicted by DFT is due to the increase in the populations of acoustic phonons at room temperature (Fig. 2, black curves). However, as already mentioned, it cancels out when the
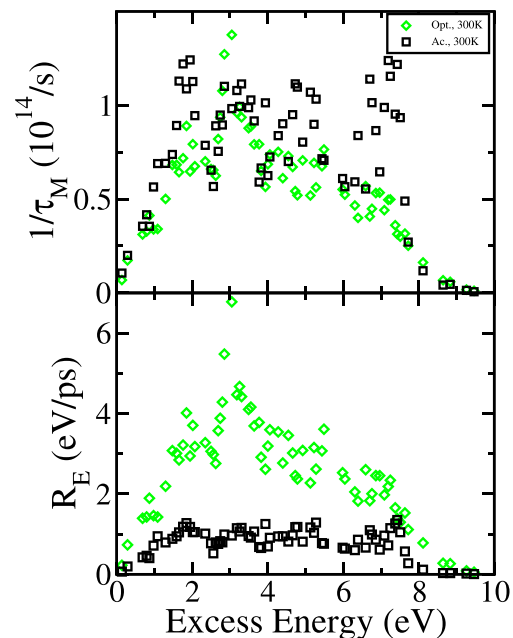
difference between emission and absorption is considered, as shown in the lower panel of Fig. 2. Indeed, as one can see in Figs. 2 and 3 (lower panels), the optical phonons are found by DFT to be the dominant channel of the energy relaxation of hot electrons in silicon at 300 K (as well as at 0 K) in agreement with the common belief.[14] Therefore, we conclude that, according to our DFT results, the main scattering channels in silicon at room temperature are different for the total scattering rates and the energy loss rates, as predicted in Ref. 14. We also note that this result does not arise from the symmetry selection rules for electron–phonon transitions between high-symmetry points and directions,[22] because the same conclusion can be drawn from the results where the initial state was chosen along the $\Gamma - X$ direction in the BZ (Fig. 2) and from the results where the average over initial state belonging to equal energy isosurfaces (see the supplementary material, Sec. I E) was made (Fig. 3).

In contrast to the DFT result, the scattering rates obtained in Refs. 9 and 11 by MC simulations predict the acoustic phonons to be dominant in the energy relaxation of the hot electrons in silicon.[9,11] Below, we discuss the main reasons for this difference.

Whereas the electron–phonon coupling constants are calculated ab initio by the DFT-based methods, contrastingly, simulations based on the MC method use a limited number of effective constants representing the main scattering channels, which are obtained by a fit of experimental data.[11,23] The choice of the main scattering channels may differ from one work to another. Because of this, the effective constants representing electron–phonon scattering may differ considerably

in different works. Tables comparing available data for silicon can be found, e.g., in Refs. 6 and 11. In Ref. 11, one can find a table comparing the effective constants, which describe the intravalley electron–phonon scattering as well as the intervalley electron–phonon scattering between Δ valleys used in various works based on MC simulations. In Ref. 6, a table comparing the DFT results to the other effective constants, which describe the intervalley electron–phonon scattering between Δ valleys of the lowest conduction band (CB), can be found.

One must note that some experimental information is available only for the long-wavelength electron–phonon coupling constants (intravalley deformation potentials):[24,25] tables comparing the available theoretical and experimental data for intravalley acoustic deformation potentials in silicon were published in Refs. 26–28. In contrast, unfortunately, there is no experiment which can distinguish between different short-wavelength (intervalley) electron–phonon scattering channels for hot electron relaxation, so that such an information always comes from theory. The experimentally determined values of the effective electron–phonon scattering constants, which can be found in the literature, are determined indirectly from transport or spectroscopy data and depend heavily on the models used to fit the experimental data (e.g., the number and the nature of the main channels).[26] At the same time, short-wavelength (intervalley) scattering represents the main scattering channel for electrons excited above the second CB minimum,[8,13] which is the case under discussion in the present work. Therefore, no reliable experimental data can be added to the discussion of the values of the (mostly intervalley) electron–phonon coupling constants for highly excited electrons which follows below.

Note also that the values of the electron–phonon matrix elements in silicon obtained with DFT-based calculations over various directions in the BZ were shown and discussed in Ref. 3. Overall, our DFT-based results are found, as expected, to be very similar to the ones of Ref. 3 and to other previous DFT-based works.[2,4] One must note that in this work, we do not take into account the quadrupolar interaction[2,29,30] in the Wannier interpolation (see the supplementary material, Sec. I C).

We next discuss the effective values of the electron–phonon coupling constants for highly excited electrons, which differ, e.g., from the values at the bottom of the first CB which were discussed in Ref. 6. Following Ref. 11, no explicit distinction is made for scattering between different valleys and/or short/long wavelength scattering. The effective DFT-based values of the electron–phonon coupling constants presented here in Table I were obtained by a fit on our calculated total electron–phonon scattering rates for the initial state in the lowest conduction band and in the second conduction band at excess energy that ranges between 1 and 3 eV, using the same models as the ones used in Ref. 11: for acoustic modes, the electron–phonon deformation potentials in Eq. (1) were replaced by $\Delta_{acc} \cdot q$, and for optical modes, by a constant D_{opt}. Note that deformation potentials $D_{mn\nu}$, usually discussed in the literature, and the electron–phonon matrix elements $g_{mn\nu}$ of Eq. (1) are related simply by a proportionality coefficient: $D_{mn\nu}(\mathbf{k}, \mathbf{q}) = \sqrt{2M\omega_{\mathbf{q}\nu}} g_{mn\nu}(\mathbf{k}, \mathbf{q})$,[31] where M is the mass of the unit cell.[31]

While fitting the effective electron–phonon coupling constants to reproduce the *ab initio* result of Eq. (1), the DFT-based descriptions of the band structure and the phonon dispersion were left unchanged; therefore, no effective mass model was necessary for the fit.

The DFT-based effective electron–phonon parameters for the highly excited electrons in silicon, obtained with the above-described method, are shown in the first column of Table I.

TABLE I. Effective parameters of the electron–phonon coupling in the CB of silicon, adjusted from the total electron–phonon scattering rates calculated by DFT at 300 K, with the same models as those of Refs. 11 and 32, compared to parameters from Refs. 11 and 32 (see the text).

	This work (DFT)	From Refs. 11 and 32
Lowest CB		
Δ_{acc}, TA, eV	0.9–1.0	2
Δ_{acc}, LA, eV	1.9–2.2	2
D_{opt}, TO, eV/Å	1.6–2.0	⋯
D_{opt}, LO, eV/Å	1.7–2.4	2.5
Second CB		
Δ_{acc}, TA, eV	1.2–1.3	2.5
Δ_{acc}, LA, eV	1.8–1.9	2.5
D_{opt}, TO, eV/Å	2.2–2.4	⋯
D_{opt}, LO, eV/Å	3.0–3.2	2.7

In previous DFT calculations, the electron–phonon matrix elements for transverse acoustic phonons (TA) were found to be systematically lower than the ones for the longitudinal acoustic phonons (LA), as discussed in Ref. 3. As for the optical branches, all three of them were found to provide important scattering channels for excited electrons according to the DFT results.[3] The same conclusions can be drawn from our DFT-based results as shown in Table I.

In Table I, the effective DFT-based values of the electron–phonon coupling constants are compared to the values that were used in Ref. 11, taking into account some additional details provided in Refs. 27 and 32. See Note 2 in the supplementary material for detailed explanations.

As one can see from Table I, the effective constants describing the longitudinal optical and acoustic modes (LO and LA) are quite similar in DFT and in Refs. 11 and 32. The main difference between DFT-based results and the effective constants of Ref. 11 resides in the description of transverse channels: while DFT attributes relatively less importance to TA channels, the model of Refs. 11 and 32 neglects completely the role of transverse optical (TO) channels. This difference in the description of the transverse (TA and TO) electron–phonon scattering channels between the two theoretical methods leads to the opposite conclusions concerning the roles of optical and acoustic branches in the energy loss. As already mentioned, no distinction was made for intervalley/intravalley processes, and therefore, the constants of Table I represent the effective values that contain both intervalley and intravalley contributions. However, our analysis (not shown here, see Ref. 8) shows that for highly excited electrons, the intervalley contribution is largely dominant for all scattering channels. Therefore, the difference between the two methods resides in the description of intervalley TA and TO scattering channels. From the point of view of applications, such as transport simulations, such a difference has probably very little impact, and therefore, both methods yield reliable numerical results, as shown in numerous works.[1,11]

In ==conclusion, we have shown that the rate of energy transfer from highly excited electrons to phonons has negligible temperature dependen==ce. Moreover, we have demonstrated, on the basis of DFT results, that the dominant electron–phonon scattering channels may differ for the total electron–phonon scattering rate and the energy loss rate. This fact, pointed out previously, e.g., in Ref. 14, turns out to play

an important role in silicon at room temperature. The semi-empirical Monte Carlo method of Ref. 11 and DFT-based results are found to disagree with respect to the main channels of energy transfer from hot electrons to phonons in silicon due to the important differences in the description of the electron–phonon scattering channels associated with transverse phonons. Our results showed that methods that involve a model description of the electron–phonon coupling with a limited number of channels are not suitable to provide insight into the relative importance of different electron–phonon scattering mechanisms, because the fitted effective constants are biased by the initial choice of channels. Instead, DFT-based calculations should be used to obtain information on the dominant electron–phonon scattering channels and should guide the choice of models/channels used in Monte Carlo simulations.

See the supplementary material for all technical details of our calculations. Also, Note 1 and Note 2 mentioned in the text are provided.

AUTHOR DECLARATIONS

Conflict of Interest

The authors have no conflicts of interest to disclose.

DATA AVAILABILITY

The data that support the findings of this study are available from the corresponding author upon reasonable request.

REFERENCES

[1]S. Poncé, W. Li, S. Reichardt, and F. Giustino, "First-principles calculations of charge carrier mobility and conductivity in bulk semiconductors and two-dimensional materials," Rep. Prog. Phys. **83**, 036501 (2020).

[2]G. Brunin, H. P. C. Miranda, M. Giantomassi, M. Royo, M. Stengel, M. J. Verstraete, X. Gonze, G.-M. Rignanese, and G. Hautier, "Electron–phonon beyond Fröhlich: Dynamical quadrupoles in polar and covalent solids," Phys. Rev. Lett. **125**, 136601 (2020).

[3]N. Tandon, J. D. Albrecht, and L. R. Ram-Mohan, "Electron–phonon interaction and scattering in Si and Ge: Implications for phonon engineering," J. Appl. Phys. **118**, 045713 (2015).

[4]M. Bernardi, D. Vigil-Fowler, J. Lischner, J. B. Neaton, and S. G. Louie, "Ab initio study of hot carriers in the first picosecond after sunlight absorption in silicon," Phys. Rev. Lett. **112**, 257402 (2014).

[5]J. Noffsinger, E. Kioupakis, C. G. Van de Walle, S. G. Louie, and M. L. Cohen, "Phonon-assisted optical absorption in silicon from first principles," Phys. Rev. Lett. **108**, 167402 (2012).

[6]Z. Wang, S. Wang, S. Obukhov, N. Vast, J. Sjakste, V. Tyuterev, and N. Mingo, "Thermoelectric transport properties of silicon: Towards an ab initio approach," Phys. Rev. B **83**, 205208 (2011).

[7]M. Wörle, A. W. Holleitner, R. Kienberger, and H. Iglev, "Ultrafast hot carrier relaxation in silicon monitored by phase-resolved transient absorption spectroscopy," Phys. Rev. B **104**, L041201 (2021).

[8]H. Tanimura, J. Kanasaki, K. Tanimura, J. Sjakste, and N. Vast, "Ultrafast relaxation dynamics of highly excited hot electrons in silicon," Phys. Rev. B **100**, 035201 (2019).

[9]M. V. Fischetti, P. D. Yoder, M. M. Khatami, G. Gaddemane, and L. Van de Put, "Hot electrons in Si lose energy to optical phonons: Truth or myth?," Appl. Phys. Lett. **114**, 222104 (2019).

[10]V. Talbo, J. Saint-Martin, S. Retailleau, and P. Dollfus, "Non-linear effects and thermoelectric efficiency of quantum dot-based single-electron transistors," Sci. Rep. **7**, 14783 (2017).

[11]M. V. Fischetti and S. E. Laux, "Monte Carlo analysis of electron transport in small semiconductor devices including band-structure and space-charge effects," Phys. Rev. B **38**, 9721 (1988).

[12]H. Tanimura, J. Kanasaki, K. Tanimura, J. Sjakste, N. Vast, M. Calandra, and F. Mauri, "Formation of hot-electron ensembles quasiequilibrated in momentum space by ultrafast momentum scattering of highly excited hot electrons photo-injected into the Γ valley of GaAs," Phys. Rev. B **93**, 161203–16120R (2016).

[13]J. Sjakste, N. Vast, G. Barbarino, M. Calandra, F. Mauri, J. Kanasaki, H. Tanimura, and K. Tanimura, "Energy relaxation mechanism of hot-electron ensembles in GaAs: Theoretical and experimental study of its temperature dependence," Phys. Rev. B **97**, 064302 (2018).

[14]S. Ahmad, O. P. Daga, and W. S. Khokle, "Energy and momentum loss rates for hot electrons in silicon," Phys. Status Solidi (B) **40**, 631 (1970).

[15]S. Ponce, E. R. Margine, C. Verdi, and F. Giustino, "EPW: Electron–phonon coupling, transport and superconducting properties using maximally localized Wannier functions," Comput. Phys. Commun. **209**, 116 (2016).

[16]P. B. Allen, "Theory of thermal relaxation of electrons in metals," Phys. Rev. Lett. **59**, 1460 (1987).

[17]J. Sjakste, V. Tyuterev, and N. Vast, "Intervalley scattering in GaAs: Ab initio calculation of the effective parameters for Monte Carlo simulations," Appl. Phys. A **86**, 301 (2007).

[18]J. Sjakste, K. Tanimura, G. Barbarino, L. Perfetti, and N. Vast, "Hot electron relaxation dynamics in semiconductors: Assessing the strength of the electron–phonon coupling from the theoretical and experimental viewpoints," J. Phys.: Condens. Matter **30**, 353001 (2018).

[19]S. Baroni, S. de Gironcoli, A. Dal Corso, and P. Giannozzi, "Phonons and related crystal properties from density-functional perturbation theory," Rev. Mod. Phys. **73**, 515 (2001).

[20]P. Giannozzi, O. Andreussi, T. Brumme, O. Bunau, M. Buongiorno Nardelli, M. Calandra, R. Car, C. Cavazzoni, D. Ceresoli, M. Cococcioni, N. Colonna, I. Carnimeo, A. Dal Corso, S. de Gironcoli, P. Delugas, R. A. DiStasio, Jr., A. Ferretti, A. Floris, G. Fratesi, G. Fugallo, R. Gebauer, U. Gerstmann, F. Giustino, T. Gorni, J. Jia, M. Kawamura, H.-Y. Ko, A. Kokalj, E. Küçükbenli, M. Lazzeri, M. Marsili, N. Marzari, F. Mauri, N. L. Nguyen, H.-V. Nguyen, A. Otero de-la Roza, L. Paulatto, S. Poncé, D. Rocca, R. Sabatini, B. Santra, M. Schlipf, A. P. Seitsonen, A. Smogunov, I. Timrov, T. Thonhauser, P. Umari, N. Vast, X. Wu, and S. Baroni, "Advanced capabilities for materials modelling with Quantum ESPRESSO," J. Phys.: Condens. Matter **29**, 465901 (2017).

[21]M. Calandra, G. Profeta, and F. Mauri, "Adiabatic and nonadiabatic phonon dispersion in a Wannier approach," Phys. Rev. B **82**, 165111 (2010).

[22]J. L. Birman, M. Lax, and R. Loudon, "Intervalley-scattering selection rules in III–V semiconductors," Phys. Rev. **145**, 620 (1966).

[23]C. Jacoboni and L. Reggiani, "The Monte Carlo method for the solution of charge transport in semiconductors with applications to covalent materials," Rev. Mod. Phys. **55**, 645 (1983).

[24]D. D. Nolte, W. Walukiewicz, and E. E. Haller, "Band-edge hydrostatic deformation potentials in III–V semiconductors," Phys. Rev. Lett. **59**, 501 (1987).

[25]G. S. Argill, J. Angilello, and K. L. Kavanagh, "Lattice compression from conduction electrons in heavily doped Si:As," Phys. Rev. Lett. **61**, 1748 (1988).

[26]J. Sjakste, I. Timrov, P. Gava, N. Mingo, and N. Vast, "First-principles calculations of electron–phonon scattering," in *Annual Review of Heat Transfer* (Begell House Inc., Danbury, CT, 2014), Vol. 17, p. 333.

[27]M. V. Fischetti and S. E. Laux, "Band structure, deformation potentials, and carrier mobility in strained Si, Ge, and SiGe alloys," J. Appl. Phys. **80**, 2234 (1996).

[28]J. T. Teherani, W. Chern, D. A. Antoniadis, J. L. Hoyt, L. Ruiz, C. D. Poweleit, and J. Menéndez, "Extraction of large valence-band energy offsets and comparison to theoretical values for strained-Si/strained-Ge type-II heterostructures on relaxed SiGe substrates," Phys. Rev. B **85**, 205308 (2012).

[29]V. A. Jhalani, J.-J. Zhou, J. Park, C. E. Dreyer, and M. Bernardi, "Piezoelectric electron–phonon interaction from *ab initio* dynamical quadrupoles: Impact on charge transport in wurtzite GaN," Phys. Rev. Lett. **125**, 136602 (2020).

[30]S. Poncé, F. Macheda, E. Margine, N. Marzari, N. Bonini, and F. Giustino, "First-principles predictions of hall and drift mobilities in semiconductors," Phys. Rev. Res. **3**, 043022 (2021).

[31]S. Zollner, S. Gopalan, and M. Cardona, "Microscopic theory of intervalley scattering in GaAs: K-dependence of deformation potentials and scattering rates," J. Appl. Phys. **68**, 1682 (1990).

[32]M. Fischetti, N. Sano, S. Laux, and K. Natori, "Full-band-structure theory of high-field transport and impact ionization of electrons and holes in Ge, Si, GaAs, InAs, and InGaAs," Res. Gate (published online 2015).

[33]G. Pizzi, V. Vitale, R. Arita, S. Blügel, F. Freimuth, G. Géranton, M. Gibertini, D. Gresch, C. Johnson, T. Koretsune, J. Ibañez-Azpiroz, H. Lee, J. M. Lihm, D. Marchand, A. Marrazzo, Y. Mokrousov, J. I. Mustafa, Y. Nohara, Y. Nomura, L. Paulatto, S. Poncé, T. Ponweiser, J. Qiao, F. Thöle, S. S. Tsirkin, M. Wierzbowska, N. Marzari, D. Vanderbilt, I. Souza, A. A. Mostofi, and J. R. Yates, "Wannier90 as a community code: New features and applications," J. Phys.: Condens. Matter **32**, 165902 (2020).